

Full Length Research Paper

# Expression, purification and characterization of *Oryza sativa* L. NAD-malic enzyme in *Escherichia coli*

Hao Zhou<sup>1</sup>, Shenkui Liu<sup>2</sup> and Chuanping Yang<sup>1\*</sup>

<sup>1</sup>State Key Laboratory of Forest Tree Genetic Improvement and Biotechnology, Northeast Forestry University, Harbin, 150040, Heilongjiang Province, P.R. China.

<sup>2</sup>Alkali Soil Natural Environmental Science Center (ASNEC), Northeast Forestry University, Harbin, 150040, Heilongjiang Province, P.R. China.

Accepted 26 August, 2011

The cDNA fragment of a rice *NAD-malic enzyme* (*OsNAD-ME<sub>1</sub>*) was cloned and constructed into expression vector (pGEX-6p-3). *OsNAD-ME<sub>1</sub>* was successfully expressed as a GST fusion protein in *Escherichia coli* BL21. The optimal concentration of IPTG for inducement was 1 mmol/L and the optimal culture temperature was 30°C. The fusion protein was purified by using affinity chromatography with a glutathione sepharose 4B column. After enzymatic cleavage of GST tag, the *OsNAD-ME<sub>1</sub>* recombinant protein was collected for studying its kinetic properties. The optimum pH and temperature for catalytic reaction of *OsNAD-ME<sub>1</sub>* were pH 6.4 and 35°C, respectively. The  $k_{cat}$  value determined at pH 6.4 was 36.38 s<sup>-1</sup> and the  $K_m$  values for NAD<sup>+</sup> and malate were 0.10 and 15.98 mmol/L, respectively. The maximum activity of *OsNAD-ME<sub>1</sub>* using NADP<sup>+</sup> as coenzyme was 64.47% of that using NAD<sup>+</sup> as coenzyme.

**Key words:** Enzyme activity, GST fusion protein, kinetic properties, NAD-malic enzyme, *Oryza sativa* L., purification.

## INTRODUCTION

Malic enzymes (MEs) widely distributed in nature, have been identified in different organisms, such as bacteria, yeast, fungi, plants, animals and humans. MEs catalyze the oxidative decarboxylation of L-malate to pyruvate in the presence of cations (typically Mg<sup>2+</sup> or Mn<sup>2+</sup>) with the concomitant reduction of coenzyme NAD<sup>+</sup> or NADP<sup>+</sup> (L-malate + NAD(P)<sup>+</sup> → Pyruvate + CO<sub>2</sub> + NAD(P)H + H<sup>+</sup>) (Chang and Tong, 2003). Based on their coenzyme specificities and abilities to decarboxylate oxaloacetate (OAA), MEs can be divided into three categories: EC 1.1.1.38 (NAD<sup>+</sup> dependent; decarboxylates OAA), EC 1.1.1.39 (prefers NAD<sup>+</sup> rather than NADP<sup>+</sup>; does not decarboxylate OAA) and EC 1.1.1.40 (NADP<sup>+</sup> dependent; decarboxylates added OAA) (Fukuda et al., 2005; Bologna et al., 2007). Plant NAD-malic enzymes (NAD-MEs) including NAD-MEs from *Oryza sativa* L. (*OsNAD-MEs*) belong to the EC 1.1.1.39 subtype, as they are not able to decarboxylate OAA (Maurino et al., 2009).

Their amino acid sequences are also highly conserved among a large number of organisms, suggesting that MEs have important biological functions. In plants, the substrates and products of them are involved in diverse metabolic pathways such as photosynthesis and respiration (Maurino et al., 2009). Moreover, it was considered that plant NADP-malic enzymes (NADP-MEs) were involved in plant defense responses. Plant *NADP-MEs* were induced by many biotic or abiotic stresses, such as pathogen (Sutherland, 1991), wounding, UV-B radiation (Casati et al., 1999), ABA, SA, low temperature, dark, salt and drought stress (Fu et al., 2009). The mechanism about stress resistance was postulated that the enzyme was implicated in defense-related deposition of lignin and flavonoid by providing NADPH for steps in their biosynthesis pathway requiring reductive power (Casati et al., 1999).

There is an increasing volume of available software providing location prediction information for proteins based on amino acid sequence. For instance, NAD-MEs from *Arabidopsis thaliana* (*AtNAD-MEs*) were predicted to be localized to mitochondria (Haezlewood et al., 2005,

\*Corresponding author. E-mail: yangcp\_nefu@yahoo.com.cn.  
Tel: +86-451-8219 0006. Fax: +86-451-8219 0006.

2007), which was consistent with the results revealed by a mitochondrial proteomic research (Haezlewood et al., 2004). Some C4 and crassulacean acid metabolism (CAM) plants use mitochondrial NAD-ME to decarboxylate L-malate for increasing the CO<sub>2</sub> concentration at the site of RuBisCO. In C3 plants, NAD-ME isoforms have a central function in the mitochondrial metabolism, where they are involved in L-malate respiration (Artus and Edwards, 1985). In fact, the distinction between C3 and C4 plants is not always clear-cut. Many C3 plants, meanwhile, also have several of the genes needed for C4 photosynthesis, but do not use them in the same way (Marshall et al., 2007; Duvall et al., 2003).

Plant NAD-MEs are separated into two phylogenetically related groups:  $\alpha$  and  $\beta$ . The genome of *Oryza sativa* L. possesses two genes (*OsNAD-ME<sub>1</sub>* and *OsNAD-ME<sub>2</sub>*) encoding putative NAD-MEs. *OsNAD-ME<sub>1</sub>* and *OsNAD-ME<sub>2</sub>* display 64.5% identity and belong to  $\alpha$  and  $\beta$  group, respectively. All characterized plant NAD-MEs were composed of two dissimilar subunits ( $\alpha$  and  $\beta$ ) at a 1:1 molar ratio (Tronconi et al., 2008; Willeford and Wedding, 1987; Burnell, 1987; Long et al., 1994; Winning et al., 1994). In potato and *Crassula argentea*, no activity was associated with the separated subunits (Willeford and Wedding, 1987; Winning et al., 1994), while in *A. thaliana* the subunits assembled as active homo and heterodimers both *in vivo* and *in vitro* (Tronconi et al., 2008). Under denaturing conditions, the enzyme existed as partially unfolded dimers, which were easily polymerized. Mn<sup>2+</sup> provided full protection against the polymerization (Chang et al., 2002; Chang and Chaang, 2003).

In present work, the cDNA fragment of *OsNAD-ME<sub>1</sub>* (Gene ID: 4343294) was cloned and expressed as a fusion protein in *Escherichia coli* BL21. The kinetic properties of the *OsNAD-ME<sub>1</sub>* recombinant protein including optimum temperature, optimum pH,  $k_{cat}$ ,  $K_m$  NAD and  $K_m$  malate were determined. Meanwhile, the activities with different coenzymes were determined. So far, *OsNAD-ME<sub>1</sub>* has never been over-expressed and biochemically characterized. Therefore, we would like to report the over-expression, purification and kinetic characterization of *OsNAD-ME<sub>1</sub>* recombinant protein, which will facilitate a platform for further biochemical research.

## MATERIALS AND METHODS

### Construction of expression plasmid

The cDNA fragment of *OsNAD-ME<sub>1</sub>* amplified by polymerase chain reaction (PCR) with sense primer (5'-GAATTC GAGATCGATGGCG-3', *EcoRI* site underlined) and antisense primer (5'-CTCGAGGTCTTTCTTGACAC-3', *XhoI* site underlined) was fused into the pMD-18-T (pT) vector (TaKaRa) to construct the pT-*OsNAD-ME<sub>1</sub>* plasmid. The pT-*OsNAD-ME<sub>1</sub>* plasmid DNA was digested with *EcoRI* and *XhoI*, and the digested *OsNAD-ME<sub>1</sub>* cDNA was inserted into pGEX-6p-3 vector (Amersham Pharmacia Biotech) that was digested with the same

enzymes. The recombinant plasmid was designed as pGEX-6p-3-*OsNAD-ME<sub>1</sub>* and transformed into the *E. coli* BL21.

### Expression and purification of recombinant proteins from *E. coli*

*E. coli* cells containing pGEX-6p-3-*OsNAD-ME<sub>1</sub>* plasmid were employed to produce the recombinant proteins with glutathione-S-transferase tag (GST-*OsNAD-ME<sub>1</sub>*). The cells cultured in 2×YT medium (1% yeast extract, 1.6% tryptone and 0.5% NaCl) containing 100 µg/ml ampicillin at 37°C overnight were diluted 1:100-fold with fresh pre-warmed 2×YT medium supplied with 100µg/ml ampicillin and allowed to grow with shaking (150 rpm) at 37°C. When the cell density reached OD600 of 0.8 approximately, isopropyl-β-D-thiogalactopyranoside (IPTG) was added to a final concentration of 1 mmol/L, and then the cells were cultured for additional 10 h at 30°C for inducement of the expression of GST-*OsNAD-ME<sub>1</sub>*. The cells were harvested through centrifugation at 6000 g for 5 min at 4°C and resuspended in pre-cooled lysis buffer (20 mmol/L Tris-HCl pH 8.0, 1 mmol/L EDTA, 20 mmol/L NaCl, 1% Triton X-100 and 1 mmol/L PMSF). And lysozyme (a final concentration of 1 mg/ml) was added to the suspension, which then was incubated on ice for 45 min and centrifuged at 20,000 g for 1 h. The supernatant (containing GST-*OsNAD-ME<sub>1</sub>* fusion proteins) was loaded onto a glutathione-Sepharose-4B column pre-equilibrated with buffer (20 mmol/L Tris-HCl pH 8.0, 1 mmol/L EDTA, 20 mmol/L NaCl and 1 mmol/L PMSF). Non-specifically bound proteins were removed by washing with buffer above, and the bound fusion proteins with GST tag were recovered from the resin with elution buffer (50 mmol/L Tris-HCl pH 8.0 and 10 mmol/L reduced glutathione). Enzyme purity was checked with denaturing-polyacrylamide gel electrophoresis (SDS-PAGE) and proteins were visualized with Coomassie Brilliant Blue R-250 staining. The protein concentrations were determined by the method of Bradford using BSA as standard.

### Cleavage of the GST tag

The GST-*OsNAD-ME<sub>1</sub>* fusion proteins bound to the column were digested by PreScission protease in elution buffer (50 mmol/L Tris-HCl pH 7.5 and 1 mmol/L PMSF) for 16 h at 4°C. The desired *OsNAD-ME<sub>1</sub>* recombinant proteins were collected and used for activity tests immediately or stored at minus 80°C for later use.

### Assay of *OsNAD-ME<sub>1</sub>* activity

The *OsNAD-ME<sub>1</sub>* reaction was measured by tracing NADH production. The standard reaction mixture contained 50 mmol/L Tris-HCl, 10 mmol/L MgCl<sub>2</sub>, 0.5 mmol/L NAD<sup>+</sup>, and 10 mmol/L L-malate in a final concentration. The reaction was started by adding L-malate. The absorbance at 340 nm was continuously monitored with Ultrospec 4300 pro UV/visible spectrophotometer. The product concentration was calculated by the following formula:

$$C(\text{mol/L}) = \frac{\Delta A \cdot V}{\epsilon \cdot l \cdot v}$$

Where,  $\Delta A$ ,  $V$ ,  $v$ ,  $\epsilon$  and  $l$  are the change in absorbance during reaction, the final volume, the enzymatic volume, the extinction coefficient and the width of cuvette, respectively. A molar extinction coefficient of 6220 L·mol<sup>-1</sup>·cm<sup>-1</sup> for NADH was employed in the

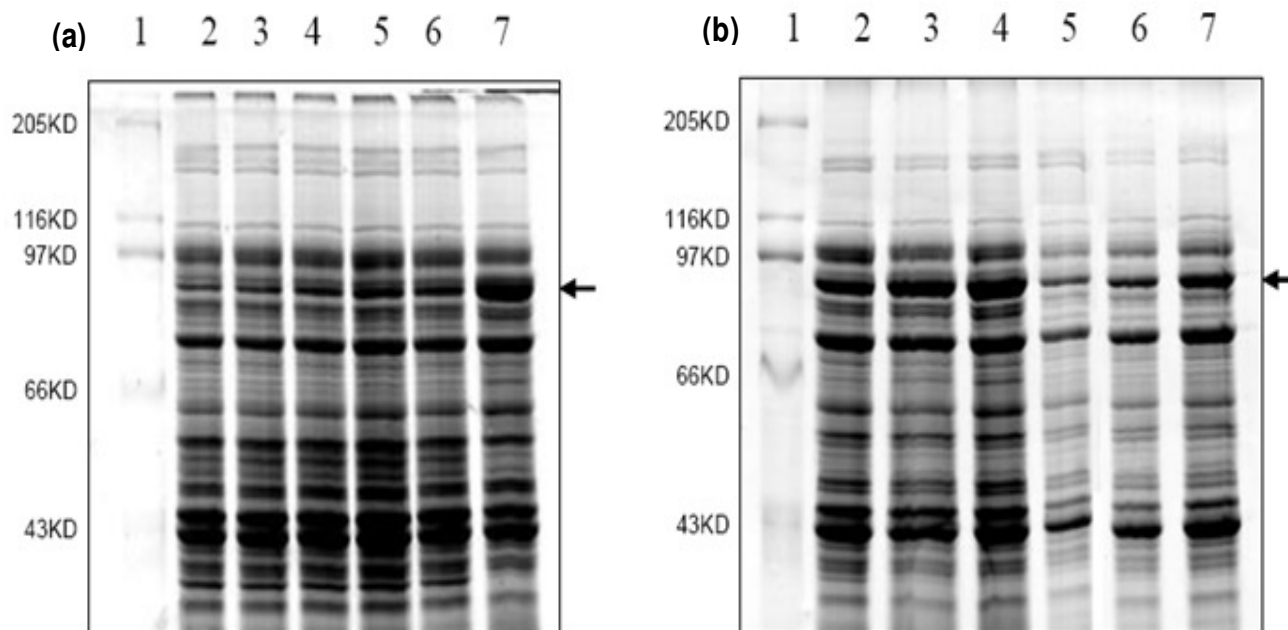


**Figure 1.** Investigation of the optimal growth conditions for the expression of GST-OsNAD-ME<sub>1</sub> fusion proteins in *E. coli* BL21. (a) Time course expressions of GST-OsNAD-ME<sub>1</sub>. Bacterial lysates were obtained from *E. coli* BL21 transformed with pGEX-6P-3-OsNAD-ME<sub>1</sub> that were induced with 1 mmol/L IPTG for different times, and were analyzed on SDS-PAGE. Lane 1, molecular weight markers; lane 2 to 7, IPTG induction for 0, 1, 3, 5, 7 and 10 h. (b) The effects of IPTG concentration and temperature on the expression of GST-OsNAD-ME<sub>1</sub>. Lane 1, the molecular weight markers. SDS-PAGE analysis of bacterial lysates were obtained from *E. coli* BL21 harboring pGEX-6P-3-OsNAD-ME<sub>1</sub> induced by different IPTG concentrations of 0.1, 0.5 and 1.0 mmol/L (Lane 2 to 4) and incubated at different temperatures of 22, 26 and 30°C (Lane 5 to 7). Arrows indicated the expressed GST-OsNAD-ME<sub>1</sub>.

calculations. One unit (katal) of enzyme activity is defined as the amount of enzyme resulting in the production of 1 mol of NADH per second. Turnover number ( $k_{cat}$ ) is defined as the maximum number of molecules of substrate that an enzyme can convert to product per catalytic site per unit of time and can be calculated as follows:

$$k_{cat}(\text{s}^{-1}) = \frac{C}{t \cdot [E]}$$

Where,  $C$ ,  $t$  and  $[E]$  are the product concentration, the reaction time and the enzyme molar concentration, respectively.

#### Kinetic studies on OsNAD-ME<sub>1</sub>

Apparent Michaelis constants ( $K_{m,malate}$  and  $K_{m,NAD}$ ) of OsNAD-ME<sub>1</sub> were determined by varying the concentration of one substrate (or coenzyme) around its  $K_m$  value and keeping the other reactants at a constant and saturating concentration. The concentrations of L-malate and NAD<sup>+</sup> were varied in the ranges of 5 to 100 and 25 to 500 μmol/L, respectively. Changes in absorbance during the time taken for the assay were linear by creating Lineweaver-Burk reciprocal plots. The y-axis ( $1/V$ ) took the reciprocal of the reaction velocity (the product yield per unit of time per unit of volume) and the x-axis ( $1/[S]$ ) took the reciprocal of the substrate concentration. The x-intercept of the graph represented  $-1/K_m$ . The  $K_m$  values of OsNAD-ME<sub>1</sub> against NAD<sup>+</sup> and L-malate were calculated, respectively. All the values were the means of three independent replications.

## RESULTS AND DISCUSSION

### Expression and purification of recombinant proteins

Expression of OsNAD-ME<sub>1</sub> as a GST fusion protein in *E. coli* BL21 cells harboring plasmid pGEX-6p-3-OsNAD-ME<sub>1</sub> was induced by IPTG. The GST-OsNAD-ME<sub>1</sub> fusion protein had a molecular mass of 88 kDa (arrow in Figure 1), which was consistent with the sum of the molecular masses of GST (26 kDa) and OsNAD-ME<sub>1</sub> (62 kDa) predicted from their nucleotide sequences.

In order to obtain enough recombinant protein for following study, optimal expression conditions were examined, including concentration of IPTG for induction together with culture temperature and time for induction. The amount of GST-OsNAD-ME<sub>1</sub> increased during the 10 h after induced by IPTG (Figure 1a) and then stabilized. It showed that the optimal culture time of cells for induction was 10 h. A range of temperature from 16 to 37°C was attempted for obtaining the optimal growth temperature. It was found that the yield of GST-OsNAD-ME<sub>1</sub> was very low at lower (below 20°C) or higher (above 30°C) temperatures. The results in Figure 1b displayed the yield of fusion proteins increased gradually in the range of 20 to 30°C, and the optimal growth temperature for the recombinant *E. coli* cells was 30°C. The effects of different IPTG concentrations,

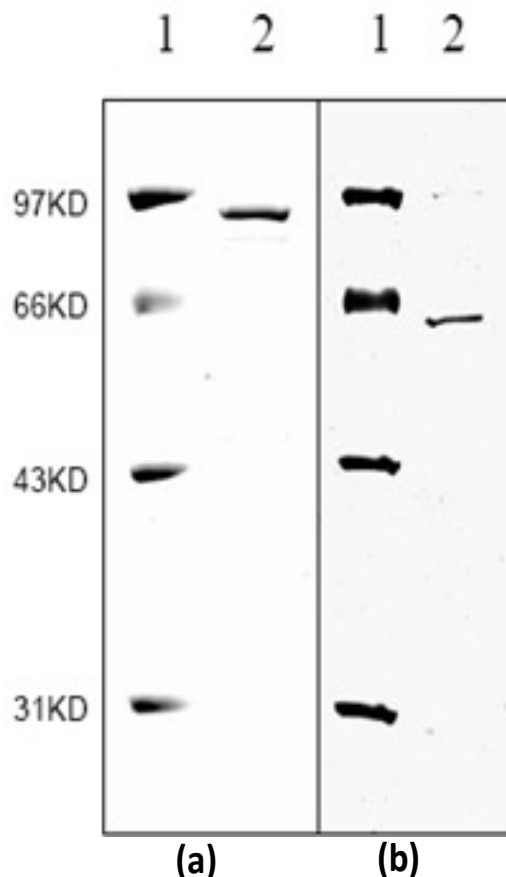


**Figure 2.** SDS-PAGE analysis of recombinant proteins purified from *E. coli* BL21. (a) and (b) Lane 1, molecular weight markers; (a) lane 2, the purified GST-OsNAD-ME<sub>1</sub>; (b) lane 2, the purified OsNAD-ME<sub>1</sub> after cleavage of GST tag

including 0.1, 0.5 and 1.0 mmol/L, on producing GST-OsNAD-ME<sub>1</sub> were determined. The results show that the expression of fusion proteins decreased at lower IPTG concentration and the optimal IPTG concentration for inducing the expression of GST-OsNAD-ME<sub>1</sub> was 1.0 mmol/L (Figure 1b).

One liter of cells was grown at 30°C and harvested by centrifugation after induced by 1.0 mmol/L IPTG for 10 h. The collected cells about 2.11 g wet weight was lysed with lysozyme. After centrifugation, the supernatant was loaded on a glutathione Sepharose 4B column. The fusion proteins specifically bound were eluted with reduced glutathione solution from the column and examined by SDS-PAGE. The GST-OsNAD-ME<sub>1</sub> homogeneous fusion proteins band (88 kDa) was obtained on SDS-PAGE (lane 2, Figure 2a). After cleavage of GST tag by PreScission Protease, the OsNAD-ME<sub>1</sub> recombinant proteins were obtained and analyzed with SDS-PAGE. As shown in Figure 2b, the recombinant proteins had molecular weight of about 62 kDa (lane 2, Figure 2b), which was consistent with the expected.

As shown in table 1, 5.78 mg purified OsNAD-ME<sub>1</sub> were obtained from 1 L of bacterial culture after two purification steps, which was enough for kinetic characterization. The total activity was 4.35  $\mu$ katal in the crude extract. The recoveries of the first purification step and second purification step were 86.28 and 70.11%, respectively. The total activity of purified OsNAD-ME<sub>1</sub> reached as high as 3.05  $\mu$ katal and the specific activity reached 527.84  $\mu$ katal/g. The activity of OsNAD-ME<sub>1</sub> remained stable for at least 8 h in the temperature about 4°C.

### Characterization of recombinant proteins

The optimum pH and temperature for the catalytic reaction of OsNAD-ME<sub>1</sub> were determined by measuring the oxidative decarboxylation of L-malate at different pH values and different temperatures under standard conditions, respectively and comparing relative enzyme activities. The relative activity of OsNAD-ME<sub>1</sub> reached

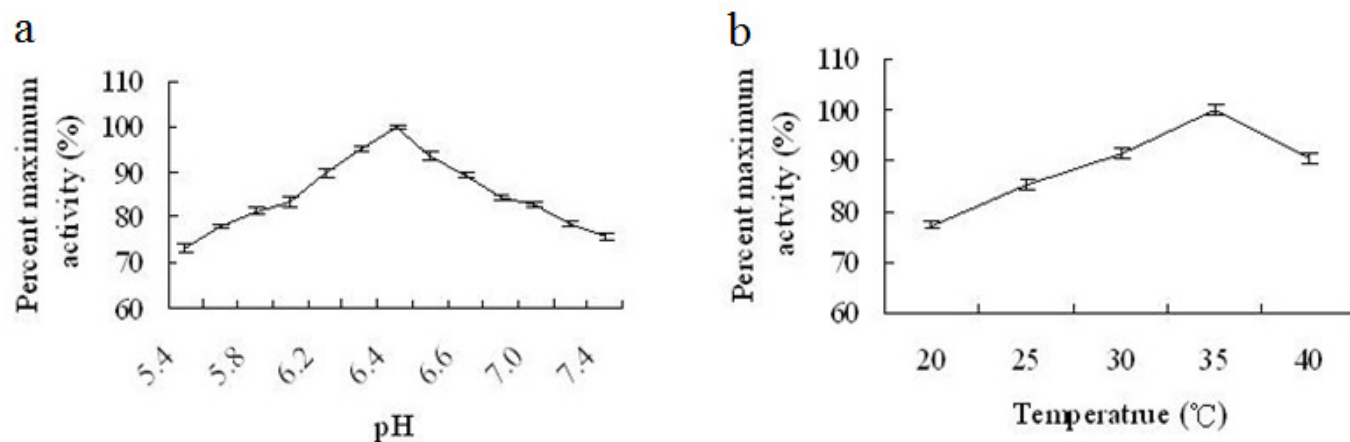


**Figure 3.** Analysis of the optimum pH and temperature of purified *OsNAD-ME*<sub>1</sub> for the catalytic reaction. (a) For the pH dependent studies, a mixture of 100 mmol/L of bis-Tris propane and 1 mol/L of HCl were used to obtain solutions with different pH by adjusting the volumes of bis-Tris propane and HCl; (b) For the temperature dependent studies, each set was treated with one temperature regime. The reaction mixture contained 50 mmol/L Tris-HCl, 10 mmol/L  $MgCl_2$ , 0.5 mmol/L  $NAD^+$  and 10 mmol/L L-malate in a final concentration at different pH values or temperatures tested. Reactions were started by the addition of L-malate. The values indicated the means of three independent replications.

maximum when the value of pH was 6.4 or the temperature was 35°C (Figure 3), thus indicating that the optimum pH was pH 6.4 and the optimum temperature was 35°C for the catalytic reaction. The optimum pH for purified *AfNAD-ME*<sub>1</sub>, belonging to  $\alpha$ -NAD-ME group as same as *OsNAD-ME*<sub>1</sub>, was reported also to be 6.4 (Tronconi et al., 2010). In prokaryote, however, the optimum pH for NAD-ME from *E. coli* K12 with regard to L-malate was 7.2 (Wang et al., 2007).

Apparent Michaelis constants of *OsNAD-ME*<sub>1</sub> were determined by altering the concentrations of one substrate and keeping the concentrations of other substrates and coenzyme at saturation. When malate was the limiting substrate (5 to 100 mmol/L) and concentration of  $NAD^+$  was 10 mmol/L, the reaction velocities of *OsNAD-ME*<sub>1</sub> were determined as shown in Figure 4a. When  $NAD^+$  was the limiting substrate (25 to 500  $\mu$ mol/L) and concentration of malate was 10 mmol/L, the reaction velocities of *OsNAD-ME*<sub>1</sub> were shown in Figure 4c. The data from Figure 4a and c were further analyzed using Lineweaver-Burk reciprocal plots (Figure 4b and d). The  $K_m$  values of *OsNAD-ME*<sub>1</sub> determined at pH 6.4 for  $NAD^+$  and malate were 0.10 and 15.98 mmol/L, respectively (Table 2). The activity of *AfNAD-ME*<sub>1</sub> in the direction of malate decarboxylation, examined at several  $NAD^+$  concentrations and at a saturating fixed level of L-malate, showed a hyperbolic response. Nevertheless, a sigmoidal behavior was observed when varying the L-malate concentration at a saturating level of  $NAD^+$  (Tronconi et al 2010). The kinetic parameters of purified *OsNAD-ME*<sub>1</sub> were described in. The  $k_{cat}$  value for *OsNAD-ME*<sub>1</sub> was 36.38  $s^{-1}$ , meanwhile, the  $k_{cat}/K_m$  values for  $NAD^+$  and malate were 357.12 and 2.28, respectively (Table 2). For comparison, the  $k_{cat}$  value of NAD-ME from *E. coli* K12 was 134.39  $s^{-1}$ . In addition, apparent  $K_{m,NAD}$

and  $K_{m,malate}$  of *EcNAD-ME* determined at pH 7.2 for L-malate and NAD were  $0.097 \pm 0.038$  and  $0.420 \pm 0.174$  mmol/L, respectively, (Wang et al., 2007).

The *OsNAD-ME*<sub>1</sub> utilized  $NAD^+$  preferentially to  $NADP^+$  as a coenzyme. When  $NADP^+$  (10 mmol/L) was used as a substrate instead of  $NAD^+$ , and the maximum activity of *OsNAD-ME*<sub>1</sub> was 64.47% of the maximum activity with  $NAD^+$  (Figure 5), which was similar with the result of NAD-ME from *Tritrichomonas foetus hydrogenosomes* using  $NADP^+$  (activity was maximal 65% of the activity with  $NAD^+$ ) (Hrdý and Mertens, 1993). However, when  $NAD^+$  (up to 4 mmol/L) was used as a substrate in place of  $NADP^+$ , neither *NADP-ME*<sub>2</sub> nor *NADP-ME*<sub>3</sub> from *O. sativa* L. showed any activity (Cheng et al., 2006). More also, Hsieh et al. (2006) showed that the single mutation of Gln362 to Lys in human mitochondrial-NAD-ME changed it to an  $NADP$ -dependent enzyme, suggesting an important role of Gln362 in the transformation of cofactor specificity. *OsNAD-ME*<sub>1</sub> is a metalloenzyme containing  $Mg^{2+}$  as a cofactor. Our results indicated that the deficiency of  $Mg^{2+}$  resulted in the failure of *OsNAD-ME*<sub>1</sub> to display any activity (Table 2). The activity of NAD-ME from *T. foetus hydrogenosomes* was also completely dependent on the presence of  $Mg^{2+}$  or  $Mn^{2+}$  (Hrdý and Mertens, 1993). During the catalytic process of malic enzyme, binding metal ion induced a conformational change within the enzyme from the open form to an intermediate form, which upon binding of L-malate, transformed further into a catalytically competent closed form (Chang et al., 2007).

Previous researches showed that *NADP-ME* expression and NADP-ME activity in rice were up-regulated by salts and osmotic stresses and rice *cytoNADP-ME* like NADP-ME in other spices played a role in enhancing tolerance of plants (Liu et al., 2007; Cheng et al., 2007;

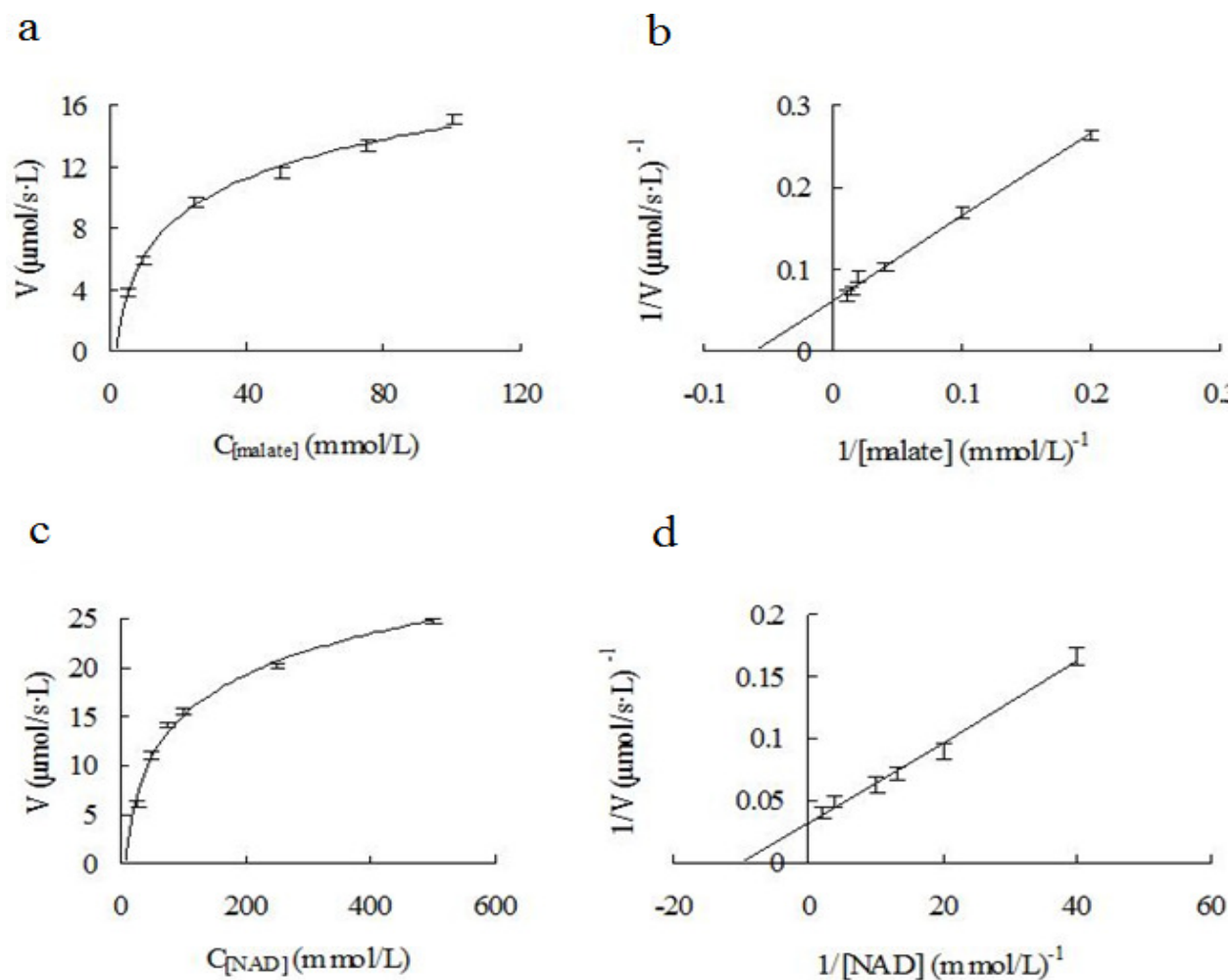


**Figure 4.** Analysis of reaction kinetics of purified *OsNAD-ME<sub>1</sub>* recombinant proteins. Assays of *OsNAD-ME<sub>1</sub>* were performed at the optimum pH 6.4. The steady-state parameters  $K_m$  were determined by fitting the data to the Michaelis-Menten equation. (a) Reaction velocities were determined by changing malate concentration in the range of 5 to 100 mmol/L with 10 mmol/L of  $NAD^+$ . (b) Lineweaver-Burk reciprocal plots of the data from (a). (c) Reaction velocity assays were carried out by changing  $NAD^+$  concentration in the range of 25 to 500  $\mu\text{mol/L}$ , and concentration of malate was 10 mmol/L. (d) Lineweaver-Burk reciprocal plots of the data from (c). The results were the means of triplicate determinations. The linear correlation coefficients of regression were 0.9953 for (b) and 0.9906 for (d).

**Table 1.** Purification of *OsNAD-ME<sub>1</sub>* recombinant proteins from *E. coli* BL21 cells.

Recombinant enzyme	Purification step	Total protein (mg)	Total activity <sup>b</sup> ( $\mu\text{katal}$ )	Specific activity ( $\mu\text{katal/g}$ )	Purification fold	Recovery (%)
<i>OsNAD-ME<sub>1</sub></i> <sup>a</sup>	Crude extract	182.05	4.35	23.90	1	100
	Soluble protein fraction	100.93	3.75	37.20	1.56	86.28
	Cleavage of GST tag	5.78	3.05	527.84	22.08	70.11

<sup>a</sup>Starting material was about 2.11 g (wet weight) of *E. coli* BL21 cultured in 1L 2×YT medium. <sup>b</sup>One unit activity of *OsNAD-ME<sub>1</sub>* was defined as the amount of enzyme resulting in the production of 1 mol of NADH per second in the standard reaction mixture containing 50 mmol/L Tris-HCl (pH 6.4), 10 mmol/L  $MgCl_2$ , 0.5 mmol/L  $NAD^+$  and 10 mmol/L L-malate

Shao et al., 2011). *OsNAD-ME<sub>1</sub>*, a member of rice NAD-dependent malic enzyme family, is estimated to perform similar biochemical and defensive function with NADP-

MEs in rice. Nevertheless, there has been no report about the tolerance of *OsNAD-ME<sub>1</sub>* to stress yet. Therefore, the results of purification and characterization

**Table 2.** Kinetic parameters of OsNAD-ME<sub>1</sub> purified from *E. coli* BL21.

Parameter	Value
Optimum pH	6.4
Optimum temperature (°C)	35
$K_{cat}^a$ (s <sup>-1</sup> )	36.38
$K_m$ NAD (mmol/L)	0.10
$K_{cat}/K_m$ NAD	357.12
$K_m$ malate (mmol/L)	15.98
$K_{cat}/K_m$ malate	2.28
Maximum activity using NADP <sup>+</sup> /NAD <sup>+</sup> (%)	64.47
Activity in the absence of Mg <sup>2+</sup>	ND <sup>b</sup>

<sup>a</sup>Measurements were made at pH 6.4; <sup>b</sup>ND, no activity was detected.

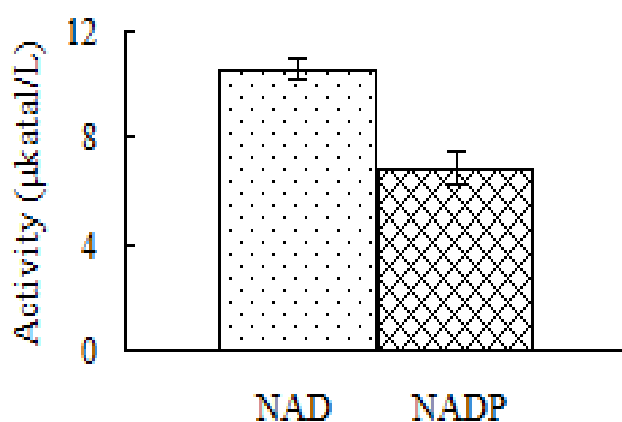


**Figure 5.** Comparison of the maximum activities of OsNAD-ME<sub>1</sub> between using NAD<sup>+</sup> and NADP<sup>+</sup> as coenzyme. The standard reaction mixture contained 50 mmol/L Tris-HCl (pH 6.4), 10 mmol/L MgCl<sub>2</sub>, 0.5 mmol/L NAD<sup>+</sup> and 10 mmol/L L-malate in a final concentration. The values indicated the means of three independent replications.

of the recombinant enzyme in this work will be beneficial to the resistance studies of OsNAD-ME<sub>1</sub> in rice.

## Conclusion

In this paper, we successfully expressed GST-OsNAD-ME<sub>1</sub> fusion proteins in *E. coli* BL21 and the optimal culture and purification procedure for generating milligram amounts of homogeneous recombinant proteins were determined. The amount of OsNAD-ME<sub>1</sub> recombinant proteins was enough for antibody production, which might be useful for future study of the function of OsNAD-ME<sub>1</sub>. The recombinant protein was active *in vitro* after the cleavage of GST tag. The  $k_{cat}$  value determined at pH 6.4 was 36.38 s<sup>-1</sup> and the  $K_m$  values for NAD<sup>+</sup> and malate were 0.10 and 15.98 mmol/L, respectively. Although, the efficiencies were different, OsNAD-ME<sub>1</sub> could use either coenzyme NAD<sup>+</sup> or NADP<sup>+</sup>.

## REFERENCES

- Artus NN, Edwards GE (1985). Properties of leaf NAD-malic enzyme from the inducible crassulacean acid metabolism species *Mesembryanthemum crystallinum*. *Plant Cell Physiol.*, 26: 341-350.
- Bologna FP, Andreo CS, Drincovich MF (2007). Escherichia coli malic enzymes: two isoforms with substantial differences in kinetic properties, metabolic regulation, and structure. *J. Bacteriol.* 189: 5937-5946.
- Burnell JN (1987). Photosynthesis in phosphoenolpyruvate carboxykinase-type C4 species: properties of NAD-malic enzyme from *Urochloa panicoides*. *J. Plant Physiol.*, 14:517-525.
- Casati P, Drincovich MF, Edwards GE, Andreo CS (1999). Malate metabolism by NADP-malic enzyme in plant defense. *Photosynth. Res.*, 61(2): 99-105.
- Chang GG, Tong L (2003). Structure and function of malic enzymes, a new class of oxidative decarboxylases. *Biochemistry* 42:12721-12733
- Chang HC, Chaang GG (2003). Involvement of single residue Tryptophan 548 in the quaternary structural stability of pigeon cytosolic malic enzyme. *J. Biol. Chem.* 278: 23996-24002.
- Chang HC, Chen LY, Lu YH, Li MY, Chen YH, Lin CH, Chang GG (2007). Metal ions stabilize a dimeric molten globule state between the open and closed forms of malic enzyme. *Biophys. J.* 93: 3977-3988.

- Chang HC, Chou WY, Chang GG (2002). Effect of metal binding on the structural stability of pigeon liver malic enzyme. *J. Biol. Chem.* 277: 4663-4671.
- Cheng YX, Long M (2007). A cytosolic NADP-malic enzyme gene from rice (*Oryza sativa* L.) confers salt tolerance in transgenic *Arabidopsis*. *Biotechnol. Lett.*, 29: 1129-1134.
- Cheng YX, Takano T, Zhang XX, Yu S, Liu DL, Liu SK (2006). Expression, purification, and characterization of two NADP-malic enzymes of rice (*Oryza sativa* L.) in *Escherichia coli*. *Protein. Expres. Purif.*, 45: 200-205.
- Duvall MR, Saar DE, Grayburn WS, Holbrook GP (2003). Complex transitions between C3 and C4 photosynthesis during the evolution of Paniceae: a phylogenetic case study emphasizing the position of *Steinchisma Hians* (Poaceae), A C3-C4 intermediate. *Plant Sci.* 164: 949-958.
- Fu ZY, Zhang ZB, Hu XJ, Shao HB, Ping X (2009). Cloning, identification, expression analysis and phylogenetic relevance of two NADP-dependent malic enzyme genes from hexaploid wheat. *C. R. Biologies*, 332: 591-602.
- Fukuda W, Ismail YS, Fukui T, Atomi H, Imanaka T (2005). Characterization of an archaeal malic enzyme from the hyperthermophilic archaeon *Thermococcus kodakaraensis* KOD1. *Archaea.* 1: 293-301.
- Haezlewood JL, Tonti-Filippini J, Verboom RE, Millar AH (2005). Combining experimental and predicted datasets for determination of the subcellular location of proteins in *Arabidopsis*. *Plant Physiol.* 139: 598-609.
- Haezlewood JL, Tonti-Filippini JS, Gout AM, Day DA, Whelan J, Millar AH (2004). Experimental analysis of the *Arabidopsis* mitochondrial proteome highlights signalling and regulatory components, provides assessment of targeting prediction programs, and indicates plant-specific mitochondrial proteins. *Plant Cell.* 16: 241-256.
- Haezlewood JL, Verboom RE, Tonti-Filippini J, Small I, Millar AH (2007). SUBA: the *Arabidopsis* subcellular database. *Nucleic Acids Res.* 35: 213-218.
- Hrdý I, Mertens E (1993). Purification and partial characterization of malate dehydrogenase (decarboxylating) from *Tritrichomonas foetus* hydrogenosomes. *Parasitology*, 107: 379-385.
- Hsieh JY, Liu GY, Chang GG, Hung HC (2006). Determinants of the Dual Cofactor Specificity and Substrate Cooperativity of the Human Mitochondrial NAD(P)<sup>+</sup>-dependent Malic Enzyme: Functional Roles of Glutamine 362. *J. Biol. Chem.* 281: 23237-23245.
- Hui CC, Gu GC (2003). Involvement of Single Residue Tryptophan 548 in the Quaternary Structural Stability of Pigeon Cytosolic Malic Enzyme. *J. Biol. Chem.*, 278: 23996-24002.
- Liu SK, Cheng YX, Zhang XX, Guan QJ, Nishiuchi S, Hase K, Takano T (2007). Expression of an NADP-malic enzyme gene in rice (*Oryza sativa* L.) is induced by environmental stresses: over-expression of the gene in *Arabidopsis* confer salt and osmotic stress tolerance. *Plant Mol. Biol.*, 64: 49-58.
- Long LL, Wang JL, Berry JO (1994). Cloning and analysis of the C4 NAD-dependent malic enzyme of amaranth mitochondria. *J. Biol. Chem.*, 269: 2827-2833.
- Marshall DM, Muhaidat R, Brown NJ, Liu Z, Stanley S, Griffiths H, Sage RF, Hibberd JM (2007). Cleome, a genus closely related to *Arabidopsis* z, contains species spanning a developmental progression from C3 to C4 photosynthesis. *Plant J.* 51: 886-896.
- Maurino VG, Gerrard Wheeler MC, Andreo CS, Drincovich MF (2009). Redundancy is sometimes seen only by the uncritical: Does *Arabidopsis* need six malic enzyme isoforms? *Plant Sci.* 176: 715-721.
- Shao HB, Liu ZH, Zhang ZB, Chen QJ, Chu LY, Brestic M (2011). Biological roles of crop NADP-malic enzymes and molecular mechanisms involved in abiotic stress. *Afr. J. Biotechnol.*, 10(25): 4947-4953.
- Sutherland MW (1991). The generation of oxygen radicals during host plant responses to infection. *Physiol. Mol. Plant Pathol.*, 39: 79-93.
- Tronconi MA, Fahnenstich H, Gerrard Wheeler MC, Andreo CS, Flügge UI, Drincovich MF, Maurino VG (2008). *Arabidopsis* NAD-Malic enzyme functions as a homodimer and heterodimer and has a major impact on nocturnal metabolism. *Plant Physiol.* 146: 1540-1552.
- Tronconi MA, Gerrard Wheeler MC, Maurino VG, Drincovich MF, Andreo CS (2010). NAD-Malic enzymes of *Arabidopsis thaliana* display distinct kinetic mechanisms that support differences in physiological control. *Biochem. J.* 430: 295-303.
- Tronconi MA, Maurino VG, Andreo CS, Drincovich MF (2010). Three different and tissue-specific NAD-malic enzymes generated by alternative subunit association in *Arabidopsis thaliana*. *J. Biol. Chem.* 285: 11870-11879.
- Wang JX, Tan HD, Zhao ZB (Kent) (2007). Over-expression, purification, and characterization of recombinant NAD-malic enzyme from *Escherichia coli* K12. *Protein Expres. Purif.*, 53:97-103
- Willeford KO, Wedding RT (1987). Evidence for a multiple subunit composition of plant NAD malic enzyme. *J. Biol. Chem.*, 262:8423-8429.
- Winning BM, Bourguignon J, Leaver CJ (1994). Plant mitochondrial NAD<sup>+</sup>-dependent malic enzyme. cDNA cloning, deduced primary structure of the 59- and 62-kDa subunit, import, gene complexity and expression analysis, *J. Biol. Chem.* 269: 4780-4786.